ISSN 0869-5911, Petrology, 2006, Vol. 14, No. 4, pp. 319–336. © Pleiades Publishing, Inc., 2006.
Original Russian Text © V.A. Zharikov, L.I. Khodorevskaya, 2006, published in Petrologiya, 2006, Vol. 14, No. 4, pp. 339–357.

Generation of Granites after Amphibolites

V. A. Zharikov and L. I. Khodorevskaya

Institute of Experimental Mineralogy, Russian Academy of Sciences, Chernogolovka, Moscow oblast, 142432 Russia

Received August 12, 2005

Abstract—This paper presents the results of a comprehensive experimental study of the formation of granitoid melts at the expense of olivine-normative amphibolites. It was shown that trondhjemite–tonalite and granite–granodiorite melts can be generated by incongruent melting reactions at pressures of 5–25 kbar at T = 800–1000°C. The compositions of coexisting phases and phase reactions were investigated in detail. It was found that interaction between these hydrous melts and the overlying peridotite material results in the metasomatic alteration of peridotites and formation of andesite melts. The granitization of amphibolite was explored. Infiltration granitization was experimentally reproduced for the first time at T = 750°C and P_f = 5 kbar. Fluid percolation through amphibolite produced a column of feldspathized and debasified rocks and granite melt completely replacing amphibolite in the proximal zone. Another extreme type of granitization occurring in amphibolite at the contact with granite melt was investigated at T = 800–950°C and P_f = 7 kbar. The diffusion of silica and alkalis resulted in the metasomatic alteration of amphibolite and formation of granitic droplets and lenses with the development of migmatite-like zones, which significantly differ in composition and structure from the zones of infiltration granitization. All the models addressed in this paper (derivation of granitoid series, interaction of granitoid melts with peridotites, and infiltration and diffusion granitization) provide insight into the mechanism of formation of many natural objects.

DOI: 10.1134/S0869591106040011

PROBLEM FORMULATION

The generation of granitoid magmas and formation of granitoid intrusions is among the key problems of geology. This is due to the relation of granitoids with the formation of many ore deposits and, more importantly, with the formation and development of the sialic crust.

Granitoids have been the focus of hundreds of studies. Some of them addressed the problems of granitoid magma genesis. Early simplified and mainly speculative concepts on the formation of granitoid magmas by crystallization differentiation of basalts, metasomatism, or anatexis of crustal rocks have been replaced by more sophisticated models based on comprehensive geochemical and experimental data. In a number of publications, we have reported experimental and natural observations bearing on the genesis of granitoids (Zharikov, 1987, 1995a, 1996a, 1996b; Zharikov and Gavrikova, 1987, 1989; Gavrikova and Zharikov, 1984; Zharikov et al., 1975, 1980, 1984, 1990, 1991, 1994; Zharikov and Khodorevskaya, 1993, 1995, 1998, 2002, 2004; Khodorevskaya and Zharikov, 1997, 1998a, 1998b, 2001; Khodorevskaya et al., 2002, 2003; Khanukhova et al., 1976a, 1976b).

Our studies allowed us to distinguish the following processes of granite formation:

(1) granitization of crustal rocks under the influence of deep (including mantle-derived) fluids;

(2) derivation of granitoid magmas from the sialic crust affected by the intrusions of basic mantle magmas;

(3) derivation of granitoid melts from mantle calcic eclogites owing to the decomposition (at decreasing T and P) of silica-oversaturated clinopyroxene;

(4) generation of granitoid melts from amphibolites (metamorphosed mantle-derived basic rocks) at the expense of their incongruent partial melting.

Note that these mechanisms of granite formation operate simultaneously or in sequence during the evolution of the Earth's crust depending on the geodynamic conditions and depth level.

All these mechanism have received experimental support, mainly from our studies, the most important of which are cited above. However, of particular interest are the problems related to the generation of granitoids under mantle conditions and after mantle rocks.

In the 1970s, we synthesized and studied high-pressure silica-oversaturated clinopyroxenes (Zharikov et al., 1975, 1980, 1984; Khanukhova et al., 1976a, 1976b). Within the pressure range 25–60 kbar, they contain up to 20–55% of the $Ca_{0.5}AlSi_3O_8$ molecule or 8–20 mol % excess silica. The decomposition of silica-oversaturated clinopyroxenes (in response to cooling and decompression) with the release of free SiO_2 strongly depresses eutectic temperature and results in the formation of silica-saturated granitoid magmas (their composition depends on the degree of melting). The existence of high-pressure silica-oversaturated cli-

nopyroxenes was confirmed by experimental studies of other authors (e.g., Gasparik, 1984, 1986; Surkov and Kuznetsov, 1996; Surkov and Doroshev, 1998). However, this model of granitoid magma generation in the mantle has received little attention.

The models of granitoid series formation by the melting of olivine-normative amphibolites (mantle metabasic rocks) in subduction zones and by the granitization of amphibolites under the *P–T* parameters of the lower crust have been much more extensively studied, both experimentally and theoretically. This paper presents an overview of our experimental investigations of the melting and granitization of amphibolites under high *T–P* parameters. Taking into account the limited volume of a journal paper, most of the obtained results are presented in diagrams. The relevant analytical data can be found in the aforementioned publications.

MELTING OF AMPHIBOLITES AT PRESSURES OF 5–25 KBAR

Before our studies, the melting of amphibolites had been investigated by Rushmer (1991), Beard and Lofgren (1991), Rapp et al. (1991), Wolf and Wyllie (1986, 1991, 1993), Winther and Newton (1991), and Hacker (1990).

We performed several experimental series on the melting of amphibolite corresponding to the composition of typical olivine-normative metabasalt (wt %): 47.59 SiO_2, 1.37 TiO_2, 13.39 Al_2O_3, 12.43 FeO, 0.06 MnO, 7.67 MgO, 11.21 CaO, 3.06 Na_2O, 0.92 K_2O, 0.49 P_2O_5, 0.13 Cl, and a total of 98.32; its CIPW normative composition is the following (wt %): 5.44 *Kfs*, 18.68 *Ab*, 20.08 *An*, 3.91 *Ne*, 26.82 *Di*, 18.52 *Ol*, and 2.60 *Ilm*.[1] The samples were composed of 70–75% amphibole with the following composition (wt %): 40.80 SiO_2, 2.17 TiO_2, 11.47 Al_2O_3, 17.22 FeO, 0.19 MnO, 9.57 MgO, 11.25 CaO, 2.62 Na_2O, 1.46 K_2O, 0.80 Cl, ≈2.0 H_2O (LOI), and a total of 99.55; and 25–30% An_{46} plagioclase containing (wt %) 56.61 SiO_2, 0.04 TiO_2, 26.51 Al_2O_3, 9.46 CaO, 6.40 Na_2O, 0.08 K_2O, and a total of 99.10.

The experiments were carried out under "dry" conditions, that is, under natural water content in the amphibolite, at *T* of 800, 900, and 1000°C and P_{tot} of 5, 14, 20, and 25 kbar. In addition to these series, the influence of fluids was experimentally explored at P_f = 5 and 7.5 kbar in the presence of H_2O or H_2O + HCl, H_2O + NaCl, H_2O + KCl, and H_2O + $CaCl_2$ fluids.

The compositions of melts (quenched glasses) and solid phases were determined by electron microprobe analysis on Camebax (Institute of Experimental Mineralogy, Russian Academy of Sciences) and CamScan with EOS Link An10/85S (Petrology Department, Moscow State University). Usually 10–12 measurements were performed for the calculation of one average representative analysis, which was used for further calculations and inferences. The analytical error was usually less than 10%, and could be higher (no more than 30%) only for the analysis of alkalis in small glass samples.

Figure 1 summarizes the *T–P* phase relations of "dry" amphibolite melting. This diagram illustrates main regular variations in the mineral composition of residues depending on temperature and pressure. Pyroxenes appear in the residues at increasing temperature and pressure; plagioclase is replaced by garnet with increasing pressure; and hornblende disappears at pressures of more than 20 kbar, being completely replaced by the assemblage *Opx* + *Cpx* + *Grt*.

Of special interest for the purposes of this paper is the temperature and pressure dependence of the composition of melts formed by partial melting of amphibolite. Table 1 presents the chemical composition and CIPW norms of quenched glasses from the experimental products. Figure 2 presents the albite–anorthite–potassium feldspar diagram for the normative compositions of melts obtained both under dry conditions at *P* of 5, 14, 20, and 25 kbar and in the presence of water (at P_{H_2O} of 5 and 7.5 kbar) or H_2O + 1 M HCl solution (P_f = 5 kbar). Figure 3 shows the normative compositions of melts obtained in the same experiments under dry and water-saturated conditions projected onto the quartz–albite–potassium feldspar plane. Figures 4 and 5 show the compositions of solid phases coexisting with the melts.

The following relationships deserve special attention.

(1) Note primarily that silica-saturated granitoid melts were formed in all melting experiments at temperatures above the solidus of water-saturated olivine tholeiite (i.e., at 800, 900, and 1000°C). This was observed both under dry conditions at *P* of 5, 14, 20, and 25 kbar, i.e., under the water content of natural amphibolites, and in the water-saturated system (P_{tot} = P_f = 5 and 7.5 kbar). It is worth noting that the experimental results confirmed the theoretical inference of Zharikov (1995a, 1995b) on the inconsistency of the model of dehydration melting (e.g., Thompson, 1982). We demonstrated that free water appears in dry systems owing to amphibole dehydration, and partial melting begins when the temperature reaches the water-saturated solidus. Thus, the *P–T* conditions of amphibolite melting under dry and water-saturated conditions are identical. The difference is only in the amount and in part in the composition of resulting melt owing to the different thermodynamic regimes of H_2O.

(2) There is a clear temperature dependency of the amount and silica content of partial melt. Small

[1] Mineral abbreviations: *Ab*, albite; *An*, anorthite; Pl_{46}, plagioclase with 46% anorthite component; *Kfs*, potassium feldspar; *Ne*, nepheline; *Di*, diopside; *Ol*, olivine; *Ilm*, ilmenite; *Ap*, apatite; *Hbl*, hornblende, amphibole; *Cpx*, clinopyroxene; *Opx*, orthopyroxene; *Grt*, garnet; *Hy*, hypersthene; *Qtz*, quartz; *Crd*, corundum; and *L*, glass (melt).

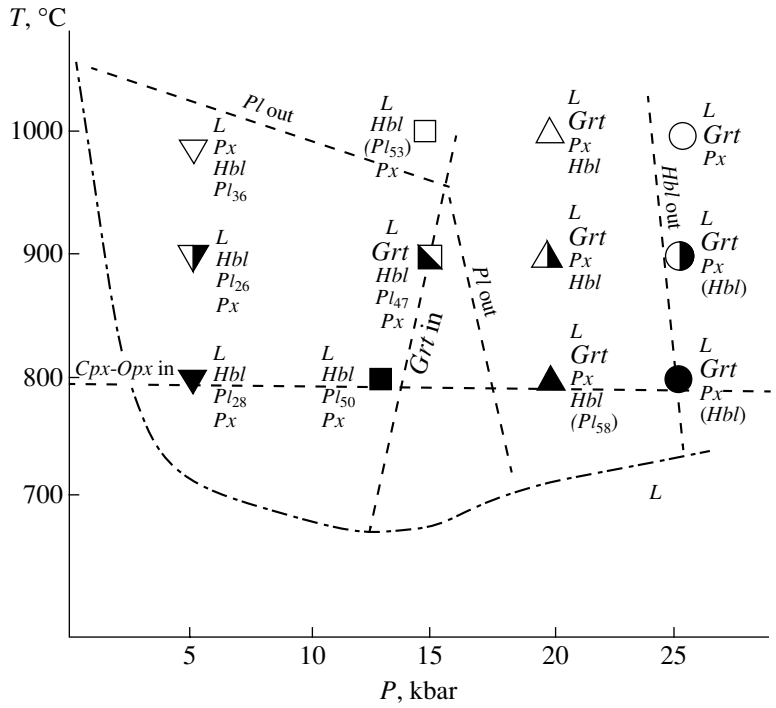

Fig. 1. Generalized *T–P* phase diagram for experiments on the melting of amphibolites under dry conditions. Titanomagnetite occurs in the residues together with other minerals. Symbols in parentheses indicate apparently metastable minerals. The dash–dot line is the liquidus of fluid-saturated olivine-bearing tholeiite (Yoder, 1962; Wyllie, 1979) at $P = P_{H_2O}$; the dashed lines correspond to the disappearance (out) and appearance (in) of particular phases in the residues.

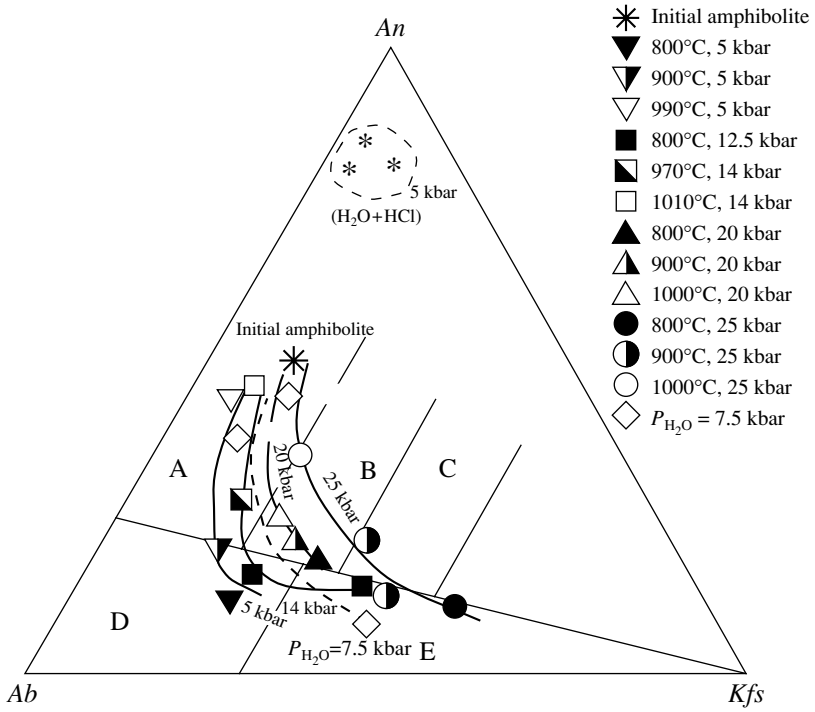

Fig. 2. Albite–anorthite–orthoclase diagram for the normative compositions of melts formed by the partial melting of amphibolites. Fields: A, tonalites; B, granodiorites; C, quartz monzonites; D, trondhjemites; and E, granites. The solid lines show variations in melt composition under dry conditions at pressures of 5, 14, 20, and 25 kbar, and the dashed lines correspond to H_2O-saturated experiments at 5.0 and 7.5 kbar. The field of melts formed in experiments with H_2O + 1 M HCl solution is strongly shifted to the anorthite apex.

Table 1. Chemical compositions (wt %) and CIPW norms of partial melts (quenched glasses)

Run no.	*T*, °C	*P*, kbar	Fluid	SiO_2	Al_2O_3	FeO	MgO	CaO	Na_2O	K_2O	Total*	*Qtz*	*Kfs*	*Ab*	*An*	*Di*	*Hy*	*Crd*
Amphibolite				49.40	13.90	12.96	7.96	11.64	3.18	0.96	98.31							
C-11	800	5	–	72.61	15.36	1.19	0.15	2.51	5.63	2.55	94.81	24.23	15.07	47.64	9.11	2.91	1.04	–
C-14	900	5	–	68.00	18.15	1.58	0.31	3.71	5.78	2.45	95.07	15.83	14.42	48.74	16.33	1.74	2.38	–
C-13	990	5	–	60.02	24.21	1.21	0.77	7.30	5.71	0.78	97.59	6.02	4.61	48.31	36.21	–	4.14	0.70
A-3	800	12.5	–	70.64	13.36	4.72	1.59	2.37	3.20	2.14	95.78	25.26	24.35	27.08	9.92	1.56	11.84	–
A-2	880	14	–	69.97	18.72	1.29	0.00	1.92	5.41	2.69	97.86	23.02	15.90	45.77	9.52	–	2.37	3.42
A-8	920	14	–	65.54	20.05	1.37	0.06	5.18	5.60	2.21	95.93	12.75	13.06	47.38	23.04	2.34	1.43	–
A-18	1000	14	–	57.43	25.35	1.21	0.00	9.81	5.75	0.45	97.88	1.67	2.66	48.65	42.03	4.18	–	–
A-6	800	20	–	75.91	14.43	1.50	0.29	1.95	2.94	2.59	96.74	43.22	15.36	24.96	9.72	–	3.48	3.26
A-4	900	20	–	69.15	14.86	2.61	2.14	4.77	3.48	2.98	93.18	23.54	17.61	29.44	16.12	6.21	7.06	–
A-22	1000	20	–	61.57	15.37	4.93	3.89	9.32	2.75	2.17	100.0	8.67	14.65	38.92	17.21	12.87	7.68	–
A-9	800	25	–	74.45	15.81	1.34	1.38	1.13	1.81	4.07	82.74	42.75	24.05	15.31	5.61	–	5.90	6.38
A-19	900	25	–	71.41	16.79	1.84	0.29	1.42	3.47	4.79	100.0	27.88	28.30	29.36	7.04	–	4.10	3.32
A-7	900	25	–	72.41	15.76	1.15	0.85	3.12	2.77	3.93	89.54	32.36	23.22	23.44	15.48	–	4.23	1.28
A-20	1000	25	–	60.16	17.27	7.38	2.89	6.22	3.84	2.23	92.01	7.12	13.18	32.49	23.30	6.39	17.52	–
B-1	800	5	H_2O	74.63	14.88	1.57	0.18	1.51	3.15	3.96	85.58	36.44	23.40	26.65	7.49	–	3.33	2.69
B-8	900	5	H_2O	62.10	20.72	2.81	1.39	6.64	4.51	1.83	90.81	10.66	10.81	38.16	30.89	1.72	7.76	–
B-5	990	5	H_2O	59.45	22.35	3.17	1.47	8.14	4.17	1.25	86.84	8.52	7.39	35.28	38.57	1.52	8.72	–
B-2	800	5	HCl	72.27	16.62	2.29	1.43	6.38	0.49	0.51	75.90	49.75	3.01	4.15	31.65	–	7.77	3.66
B-3	900	5	HCl	65.52	19.77	2.49	1.42	9.44	1.13	0.23	83.71	33.64	1.36	9.56	46.83	–	8.11	0.50
B-4	990	5	HCl	61.37	21.43	2.61	2.21	11.00	1.09	0.28	86.69	25.29	1.65	9.22	52.75	1.54	9.54	–
D-3	800	7.5	H_2O	67.00	20.01	1.49	1.18	4.79	3.41	2.01	84.84	26.21	11.88	28.85	23.76	–	5.68	3.63
D-8	950	7.5	H_2O	61.44	20.03	3.06	1.90	8.49	3.37	1.71	85.14	13.36	10.10	28.51	34.48	6.36	7.18	–

* Total according to the microprobe analysis.

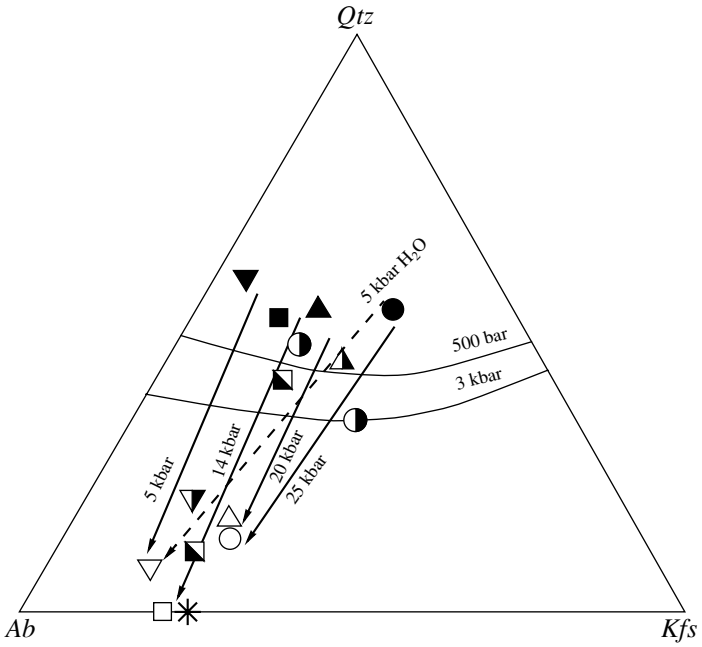

Fig. 3. Quartz–albite-orthoclase diagram for the normative compositions of melts derived by the partial melting of amphibolites. Symbols are the same as in Fig. 2.

amounts of melts with the highest SiO_2 contents are generated at low temperatures. The amount of melt increases with increasing temperature, whereas the SiO_2 concentration decreases. This is also true for water-saturated systems, but the amount of melt is higher in such a case and the composition of melt is more variable. These regular variations in melt composition are clearly seen in Figs. 2 and especially 3.

(3) The effect of pressure is most pronounced for the Na_2O/K_2O ratio, which decreases with increasing pressure. As can be seen from Figs. 2 and 3, there is a distinct tendency of the appearance of sodic trondhjemite–tonalite trends at relatively low pressure (5 and 14 kbar) and potassic peralkaline granite–quartz monzonite–granodiorite trends at higher pressures (20 and 25 kbar). At moderate pressures, there is a narrow temperature interval where tonalite melts are generated both in the dry and water-saturated systems (Fig. 2, field A). The compositions of melts formed in the presence of HCl solution plot far from other fields, near the anorthite apex (Fig. 2). This indicates that alkalis were extensively leached by acidic solutions and played a negligible role in the genesis of tonalites.

(4) Silica-saturated melts can be formed from olivine-normative amphibolites at the expense of incongruent melting reactions. The compositions of coexisting phases from a number of experiments are shown in the Na_2O–CaO–Al_2O_3 and CaO–MgO–FeO diagrams (Figs. 4, 5). It can be seen that the composition of the initial amphibolite always falls between the compositions of coexisting residual phases and melt. The incongruent melting reactions occur in different ways depending on the *P–T* conditions.

INTERACTIONS OF AMPHIBOLITE-DERIVED MELTS WITH ULTRABASIC ROCKS

The experimental results described above provided compelling evidence for the possibility of silica-saturated melt formation at high pressures by the partial melting of olivine-normative amphibolites. The general mechanism of granitoid melt formation at the expense of mantle basalts can be presented as follows:

Eruption of olivine tholeiites during oceanic crust formation	→	Amphibolite-facies metamorphism during slab descend in the zone of subduction and collision	→	Formation of trondhjemite–tonalite or granite–granodiorite melts during a further temperature increase

In order to evaluate the fate of these melts, the character of interaction between these melts and the rocks of the overlying mantle wedge must be determined at least qualitatively. To this end, we performed a series of simulation experiments.

About 900 mg of amphibolite was loaded together with distilled water (fluid/solid ratio of 1 : 3) into the lower part of a capsule. The considerable excess of amphibolite provided necessary fluid capacity with respect to the dissolved components of amphibolite. Twenty five milligrams of lherzolite was placed in the upper part of the ampoule. The experiments were car-

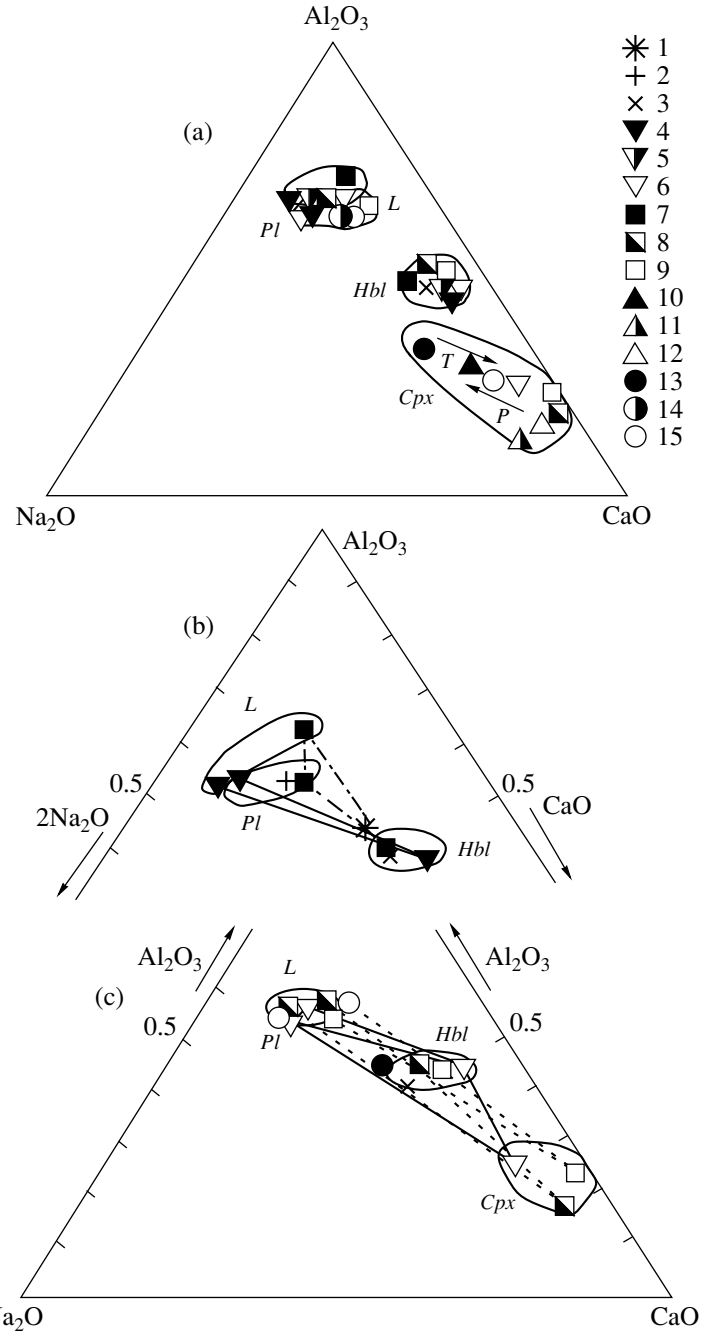

Fig. 4. (a) Diagram showing the compositions of coexisting phases in the Na_2O–CaO–Al_2O_3 coordinates and part of the $2Na_2O$–CaO–Al_2O_3 diagram at (b) 800°C and (c) 900–1000°C at pressures of 5 and 14 kbar. (1)–(3) Initial compositions of (1) amphibolite, (2) plagioclase, and (3) hornblende; (4)–(15) compositions of coexisting phases at (4) 5 kbar and 800°C, (5) 5 kbar and 900°C, (6) 5 kbar and 990°C, (7) 12.5 kbar and 800°C, (8) 14 kbar and 920°C, (9) 14 kbar and 1000°C, (10) 20 kbar and 800°C, (11) 20 kbar and 900°C, (12) 20 kbar and 1000°C, (13) 25 kbar and 800°C, (14) 25 kbar and 900°C, and (15) 25 kbar and 1000°C.

ried out at $P_{tot} = P_{H_2O} = 8$ kbar. During the experiments, the lower part of the capsule was heated to 700, 750, 800, and 850°C, and the upper part, to 1000°C, i.e., the lherzolite occurred at a higher temperature (simulating a hotter mantle wedge). In addition, similar experiments were carried out at $T = 990$°C without temperature gradient.

In order to evaluate boundary conditions, experiments were performed in the systems amphibolite + H_2O ($T = 700$–950°C and $P = 5$ and 7.5 kbar) and lherzolite + H_2O ($T = 1000$–1100°C and $P = 8$ kbar). Table 2 presents the compositions of the initial amphibolite and lherzolite and quenched glasses, i.e., melts formed from the lherzolites under the influence of fluids satu-

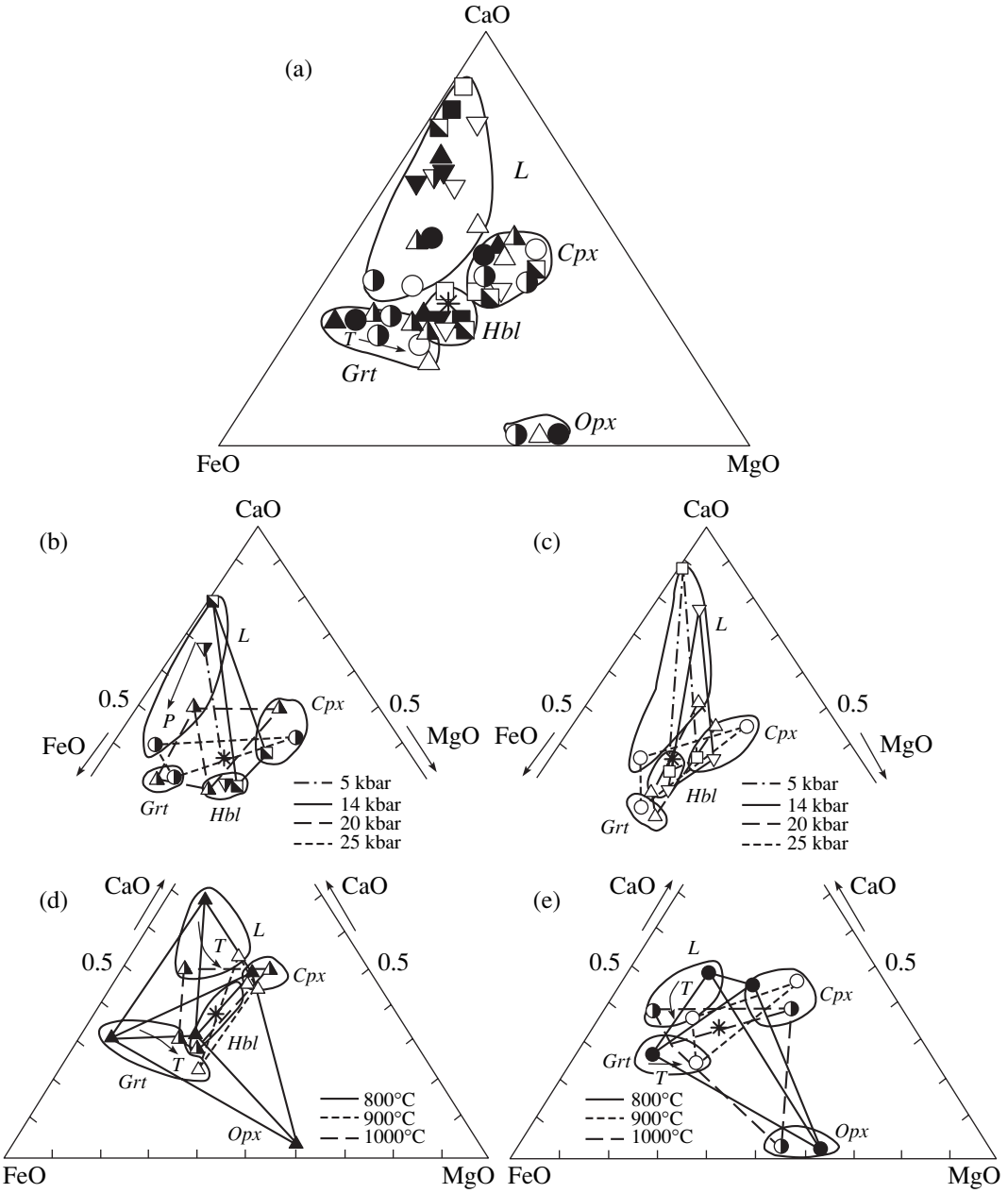

Fig. 5. CaO–MgO–FeO diagram for the compositions of experimental phases. (a) Summary diagram for P = 5–25 kbar and T = 800–1000°C. The pressure dependence of the compositions of coexisting phases at (b) T = 900°C and (c) T = 1000°C. The temperature dependence of the compositions at (d) 20 kbar and (e) 25 kbar. Symbols are the same as in Fig. 4.

rated in the components of apoamphibolite silica-rich melts. Figure 6 presents the (Na_2O + K_2O)–MgO–FeO diagram for the compositions of melts in the amphibolite/lherzolite + H_2O experiments and in the boundary systems amphibolite + H_2O and lherzolite + H_2O. Also shown are the commonly accepted petrochemical trends of the calc-alkaline and tholeiitic magmatic series (Baker and Arth, 1976).

The results of experiments in the amphibolite + H_2O boundary system are similar to those described above: silica-rich melts are formed; their compositions depend on temperature (Fig. 6); and the residues consist of hornblende, plagioclase, and at $T \geq 900$°C clinopyroxene.

A small amount of magnesian picrite melt was formed in the lherzolite + H_2O boundary system.

In the amphibolite/lherzolite + H_2O experiments, the lherzolite underwent extensive metasomatic amphibolitization and partial melting under the influence of fluid (Table 2, Fig. 6). The composition of melt approached that of andesite but showed a relatively high MgO content and, correspondingly, high MgO/FeO ratio (mantle signature in andesites). Such

Table 2. Chemical compositions (wt %) of initial amphibolite and lherzolite and quenched melts (glasses) formed after lherzolite

Oxide	1	2	3	4	5	6
SiO_2	48.66	44.62	59.88	61.98	63.75	56.94
TiO_2	1.39	0.04	0.89	0.83	0.32	0.88
Al_2O_3	13.74	1.82	22.70	18.25	22.15	19.07
FeO	12.78	7.55	1.67	2.93	1.42	5.26
MgO	7.87	42.28	1.50	2.03	1.19	2.44
CaO	11.51	3.53	10.06	8.45	9.37	9.46
Na_2O	3.12	0.13	2.18	2.85	1.74	3.28
K_2O	0.93	0.03	1.12	0.98	1.05	1.67

Note: (1) Amphibolite; (2) lherzolite; (3)–(6) glass from experiments: (3) 700/1000°C (temperatures in the lower and upper parts of the capsule are given in the numerator and denominator, respectively) and 8 kbar; (4) 800/1000°C and 8 kbar; (5) 990°C and 8 kbar; and (6) 750/1050°C and 8 kbar. The analyses were recalculated to totals of 100 wt %.

melts are formed in lherzolites under the influence of apoamphibolite fluids. The mixing of the apoamphibolite and apolherzolite melts could produce magmas with a calc-alkaline affinity, which are widespread in island-arc magmatic suites.

INFILTRATION GRANITIZATION OF AMPHIBOLITE

Of particular importance for the formation of the Earth's sialic crust is the process of granitization, which includes the metasomatic feldspathization and debasification of country rocks, their nonisochemical melting, and the replacement of altered country rocks by granitic melts. Such a model of granitization was proposed by D.S. Korzhinskii in 1952 (Korzhinskii, 1952) and has been developed in detail in our studies (Zharikov, 1987, 1996a, 1996b; Zharikov and Gavrikova, 1987, 1989; Zharikov et al., 1994; Gavrikova and Zharikov, 1984; and others), both in general theoretical aspects and by the example of the Precambrian sequences of eastern Transbaikalia. Many authors who have studied granitized rocks favored other concepts on the genesis and mechanism of granitization. The most important point distinguishing our models is the concept of a granitization column, which is formed as a result of simultaneous processes of feldspathization and debasification, nonisochemical melting, and complete replacement of altered country rocks by magmatic melt.

These concepts were supported by our experiments, which reproduced for the first time the infiltration granitization of amphibolites, i.e., formation of alteration zones in amphibolites and their replacement by melt under the influence of ascending flows of SiO_2-bearing alkaline aqueous solutions. The design of these experiments is shown in Fig. 7. An Au capsule (Fig. 7a, *1*), $50 \times 5 \times 0.2$ mm in size, was preliminarily annealed, and a circular indentation (*2*) was made on its surface at a distance of 15 or 20 mm from the bottom for the support of the sample. About 100 mg of altered haplogranite glass (*3*) was loaded into the bottom of the capsule; it served as a buffer for the saturation of fluid in granite components. The capsule was filled with 1 M HCl solution (*4*), and an amphibolite column, 4.65 ± 0.01 mm in diameter and 15 mm long (*5*), was prepared by diamond tools and tightly packed into the upper part of the capsule, where it rested on the circular indentation. A thick-walled microchamber for the collection of filtrate (*6*) was inserted into the capsule above the sample. The microchamber was manufactured from a nickel alloy and had a central hole 2 mm in diameter. The capsule was welded shut from above (*7*) and placed into a high-pressure gas apparatus. The experiment was begun from the outer pressurization of the capsule at room temperature and a pressure of 2 kbar, during which the sample was hermetically sealed by the capsule walls (Fig. 7b) preventing solution leakage. After the sealing, the experimental temperature and pressure were raised to $T = 750$°C and $P_f = 5$ kbar (during 1.5–2.0 h). The experiment lasted 95 h under such parameters, after which the sample was quenched.

The examination of experimental products revealed alterations in all amphibolite columns. Regular fluid infiltration resulted in the formation of subparallel textures in the amphibolites. Three zones of amphibolite granitization could be distinguished.

Zone I is the outer zone of biotitization and feldspathization, where primary hornblende is completely replaced by secondary biotite and, in part, by plagioclase. The secondary biotite is characterized by a higher $f_m = \frac{\sum \text{Fe}}{\text{Mg} + \sum \text{Fe}}$ value (0.52) compared with the initial biotite ($f_m = 0.43$). The plagioclase of the feldspathization zone is homogeneous (30–36% anorthite component), and relict labradorite grains ($Pl_{44–46}$) were only occasionally found. The assemblages of the outer zone are confined to the upper part of the sample.

Zone II occupies the major portion of the sample and is represented by a light-colored (at the expense of a decrease in biotite content) rock composed of secondary biotite, plagioclase, and droplets and veins of quenched melt. Platy biotite crystals are preferentially orientated parallel to the sample axis. Plagioclase occurs as elongated grains of variable size. Quenched granite melt forms droplets and veinlets among the plagioclase grains and occasionally at the contacts of plagioclase and biotite grains.

Proximal zone III is distinguished by a sharp frontal contact (with embayments) of the granite melt replacing the altered and partially resorbed amphibolites of zone II. Small relict plagioclase and ilmenite grains were occasionally observed in the granite glass at the contact with the altered amphibolite. Figure 8 presents a photograph of the lower part of one of the experimen-

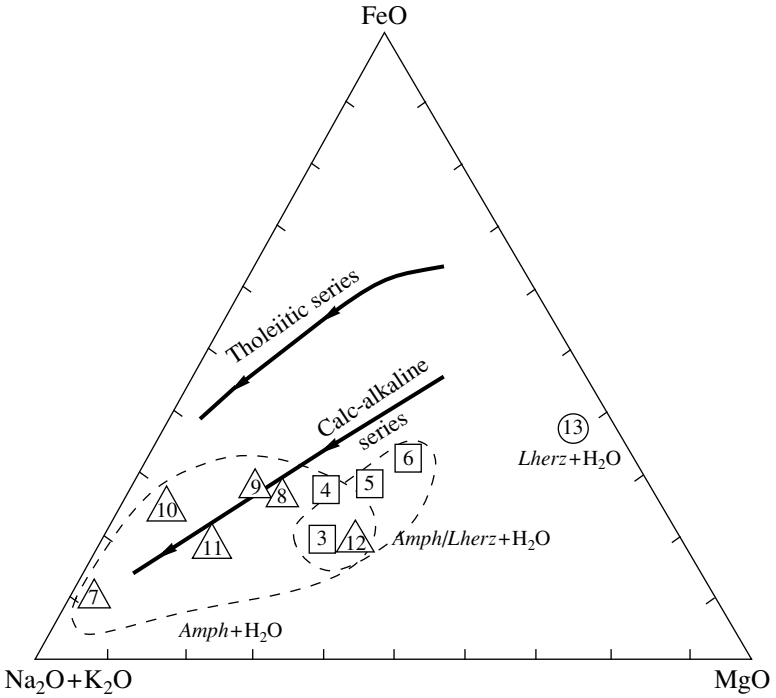

Fig. 6. Compositions of melts (quenched glasses) from melting experiments in the systems amphibolite–lherzolite–water (runs 3–6), amphibolite–water (runs 7–12), and lherzolite–water (run 13). Also shown are the trends of variations in melt composition for the tholeiitic and calc-alkaline series. Experimental parameters (*T*, °C/*P*, kbar): (3) 700–1000/8, (4) 800–1000/8, (5) 990/8, (6) 750–1050/8, (7) 800/5, (8) 900/5, (9) 990/5, (10) 700/7.5, (11) 800/7.5, (12) 950/7.5, and (13) 1000/8. *Amph*, amphibolite and *Lherz*, lherzolite.

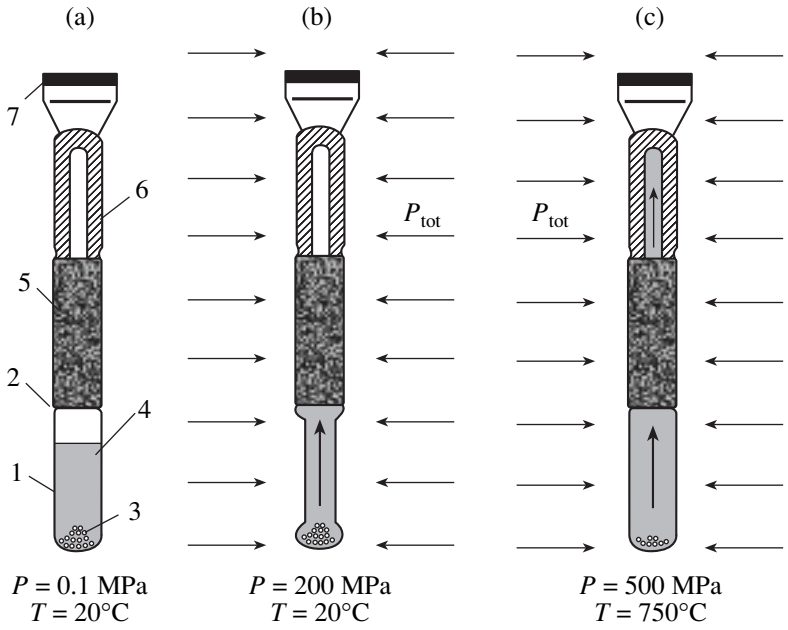

Fig. 7. A sketch of the experimental cell and conditions of infiltration granitization experiments. The arrows indicate external gas pressure in the vessel. The arrows within the ampoule show the direction of solution flow. See text for explanation.

tal samples. The sharp front of the replacement of feldspathized and debasified amphibolites by granite melt is clearly seen. The melt forms veinlets and pockets in the altered amphibolite.

The infiltration granitization of amphibolites under the experimental conditions (most importantly, under a strong pressure gradient) is obviously a disequilibrium dynamic process, approaching local equilibrium in

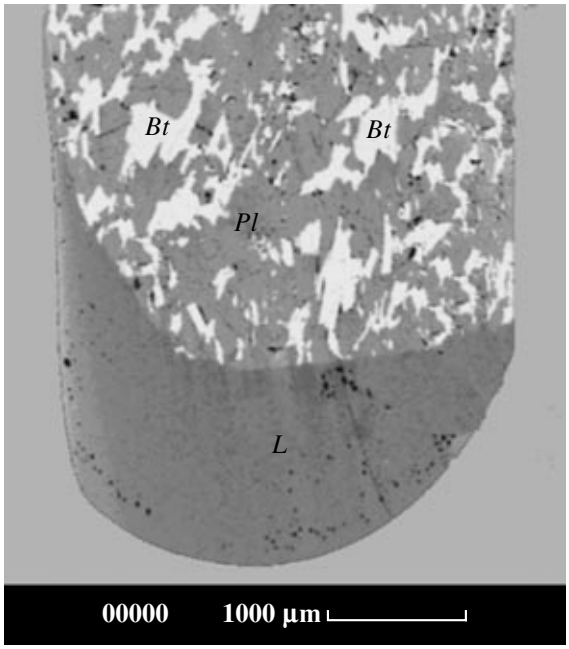

Fig. 8. Photograph of the experimental sample consisting of plagioclase (*Pl*), biotite (*Bt*), and melt (*L*).

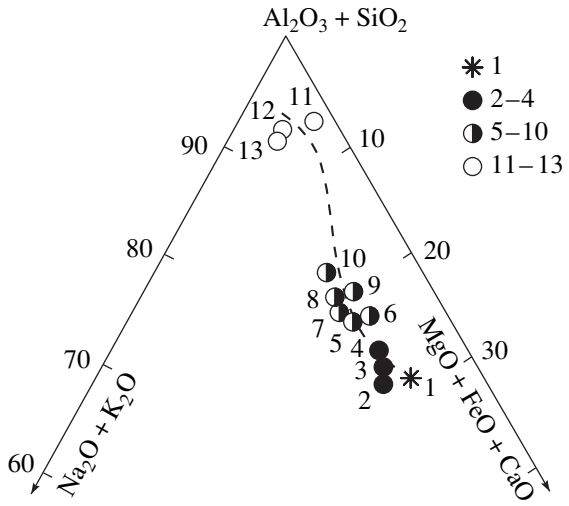

Fig. 9. Chemical compositions of initial and altered amphibolites and quenched glasses in the (Al_2O_3 + SiO_2)–(Na_2O + K_2O)–(MgO + FeO + CaO) coordinates. Symbols are explained in the text.

each zone. Figure 9 and Table 3 show the concentrations of major components in the initial (sample 1), weakly altered (zone I, samples 2–4), and strongly altered (zone II, samples 5 and 6) amphibolites and quenched granitic glasses (sample 11 from melt areas in altered amphibolites; samples 12 and 13 from the zone of pure granitic melt). The "jet" character of replacement in the altered amphibolites and the small size of the sample did not allow us to characterize the chemistry of each individual replacement zone. Samples 2–4 reflect the compositions of the least altered amphibolites, which showed only a slight increase in alkali content (feldspathization) and f_m value. The altered amphibolites are represented by samples 5–10, which are composed of biotite–plagioclase metasomatic rocks with pockets of granitic glass (samples 8–10). Finally, sample 11 is granitic melt from the altered amphibolite; the incipient granitic melts are always enriched in SiO_2. Samples 12 and 13 are granites replacing the amphibolites in the proximal zone. These observations quantitatively characterize the main tendency of infiltration granitization, which has been repeatedly noted: the debasification and feldspathization of initial amphibolites and their replacement by granitic melt.

If the dynamic column of granitization occurs under local equilibrium conditions, which is more consistent with natural systems (slower infiltration at longer time scales), its structure will be the following:

Zone of complete melting	Feldspar zone with melt	Zone of extensive feldspathization and debasification	Zone of feldspathization and debasification	Initial rock
L	$Fsp_3 + L$	$Fsp_2 + Bt_2$	$Fsp_1 + Bt_1 + Hbl$	Amphibolite
V	Al + *V*	Al + Fe	Al + Fe + Mg	

This column illustrates the general principal type of granitization zoning (lower line indicates extensive parameters for each zone).[2]

Such a granitization zoning was documented by us and other authors in many regions of the development of Late Archean and Early Proterozoic granitization. For instance, the following granitization column was observed in the Olekma zone of the Stanovoy system (Zharikov and Gavrikova, 1987):

L	*Kfs* + *L*	*Kfs* + *Pl* + *Bt*	*Pl* + *Bt* + *Hbl*	Initial amphibolite

A similar structure is characteristic of higher temperature columns after basic granulites.

[2] Note that the extensive parameters $f_{ex} = r$ define the number and varieties of phases. For instance, in the *Fsp* + *L* zone, the amount of Al controls the amount of *Fsp*, and the free volume *V*, the amount of melt.

Table 3. Average concentrations of major components (wt %) in altered amphibolites and granitic melts

Oxide	Starting amphibolite	Altered amphibolites				Altered amphibolites with granitic melts					Granitic glass	Granites from the zone of amphibolite replacement	
	1*	2	3	4	5	6	7	8	9	10	11*	12*	13*
SiO_2	51.26	48.40	48.61	49.00	51.97	52.53	53.98	52.60	52.67	55.74	77.29	77.30	75.49
Al_2O_3	18.73	19.83	19.99	19.65	21.75	21.48	22.06	21.20	21.94	22.43	15.20	13.32	14.44
FeO	8.48	10.40	9.83	8.24	6.86	6.92	6.21	5.16	5.71	3.98	1.29	1.12	0.88
MgO	4.20	5.18	5.17	4.36	3.10	3.37	3.02	1.97	2.42	1.96	0.30	0.24	0.18
CaO	8.11	3.86	4.30	5.88	5.39	5.34	4.72	7.14	5.79	5.70	2.49	1.20	1.15
Na_2O	3.52	4.65	4.16	4.44	5.18	4.65	5.84	5.67	5.27	5.98	0.65	4.17	3.18
K_2O	1.64	4.66	4.78	3.77	2.86	3.04	2.87	2.06	2.34	7.05	2.18	2.75	2.30

* Analyses were obtained on an electron microprobe by rastering the beam over areas of 400 × 400 or 800 × 800 μm.

Granitization of the Na line:

$$L \mid Pl + L \mid Pl + Hbl \mid Pl + Hbl + Cpx \parallel \text{Basic granulite}$$

Granitization of the K line (usually later than Na granitization):

L	$Kfs + L$	$Kfs + Pl$	$Pl + Hbl$	$Hbl + Pl + Cpx$	Basic schist

More examples can be readily found; some columns show specific structural features, but all of them clearly exhibit the main tendency: the initial rocks are affected by feldspathization and debasification and then transformed into extensively feldspathized and debasified rocks with pockets and veinlets of granitic melt (migmatization zone), which are completely substituted by granites formed by nonisochemical melting and replacement of the country rocks by melts (with subsequent crystallization). In order to illustrate changes in rock composition in the zones of the column, the input ($+\Delta m$) and output ($-\Delta m$) of components relative to the composition of the initial rock are shown in Fig. 10 for the experimental (Fig. 10a) and natural (Figs. 10b–10d) granitization columns. The natural data were obtained by Zharikov and Gavrikova (1987, 1989) during the investigation of granitization zones in the southern part of the Aldan–Stanovoy shield.

The granitization of amphibolites and basic granulites (*Cpx* + *Opx* + *Pl*) is widespread at lower crustal levels (under amphibolite and granulite facies conditions) in all shields. The sizes of granite bodies are variable, up to large batholith-like massifs with traces of melt movement and injection into the country rocks. The possibility of granitic melt formation through granitization under the influence of alkaline silica-rich fluids is beyond doubt and has not provoked serious objections. In contrast, some researchers were perplexed by our supposition on the mantle origin of these fluids. The question is how could the fluids generated under mantle conditions cause acidic processes, such as granitization of crustal rocks?

A series of experiments was carried out to determine the solubility of minerals at high pressures (10–50 kbar) in the "mantle" systems enstatite + H_2O, forsterite + H_2O, phlogopite + H_2O, phlogopite + orthopyroxene + H_2O, olivine + spinel + H_2O, and olivine + diopside + spinel + H_2O. These experiments and the data of other authors (Ryabchikov, 1985; Ryabchikov and Boettcher, 1986; Nakamura and Kushiro, 1974; Mysen and Kushiro, 1976; Eggler, 1983; Gorbachev, 1989; etc.) showed that considerable amounts of silicate material can be extracted by the solution at high pressures: from 15–20 to 30–40 and even 50 mol % (Fig. 11a). Furthermore, the dissolution was always incongruent: SiO_2, K_2O, and Na_2O were transported into the solution, while FeO, MgO, and CaO remained in the residue. Incongruent dissolution can be exemplified by the reaction phlogopite + $H_2O \longrightarrow$ forsterite + spinel + solution (SiO_2, K_2O, H_2O). The incongruent character of dissolution can be clearly seen in Fig. 11b. As was shown by the experimental investigations of Rb- and REE-doped materials, these lithophile elements partition into aqueous solutions at high *P–T* conditions (e.g., Irving, 1978; Flinn and Burnhem, 1979).

Another type of our experiments simulated the formation of granitoid melts in response to decompression in the basalt + H_2O system. The design and results of these experiments are shown in Fig. 12. Basalt powder was loaded into the lower part of a platinum capsule, and a plagioclase grain was suspended using a platinum wire in the upper part of the capsule. The capsule was filled with water, welded, and exposed in a high-pressure gas apparatus at P_{H_2O} = 5 kbar and T = 730°C for 24 h, after which the experiment was quenched. In some experiments, after 24 h at 5 kbar and 730°C, isothermal decompression was simulated: the experimental pressure was decreased to 2.0–3.5 kbar, and the cap-

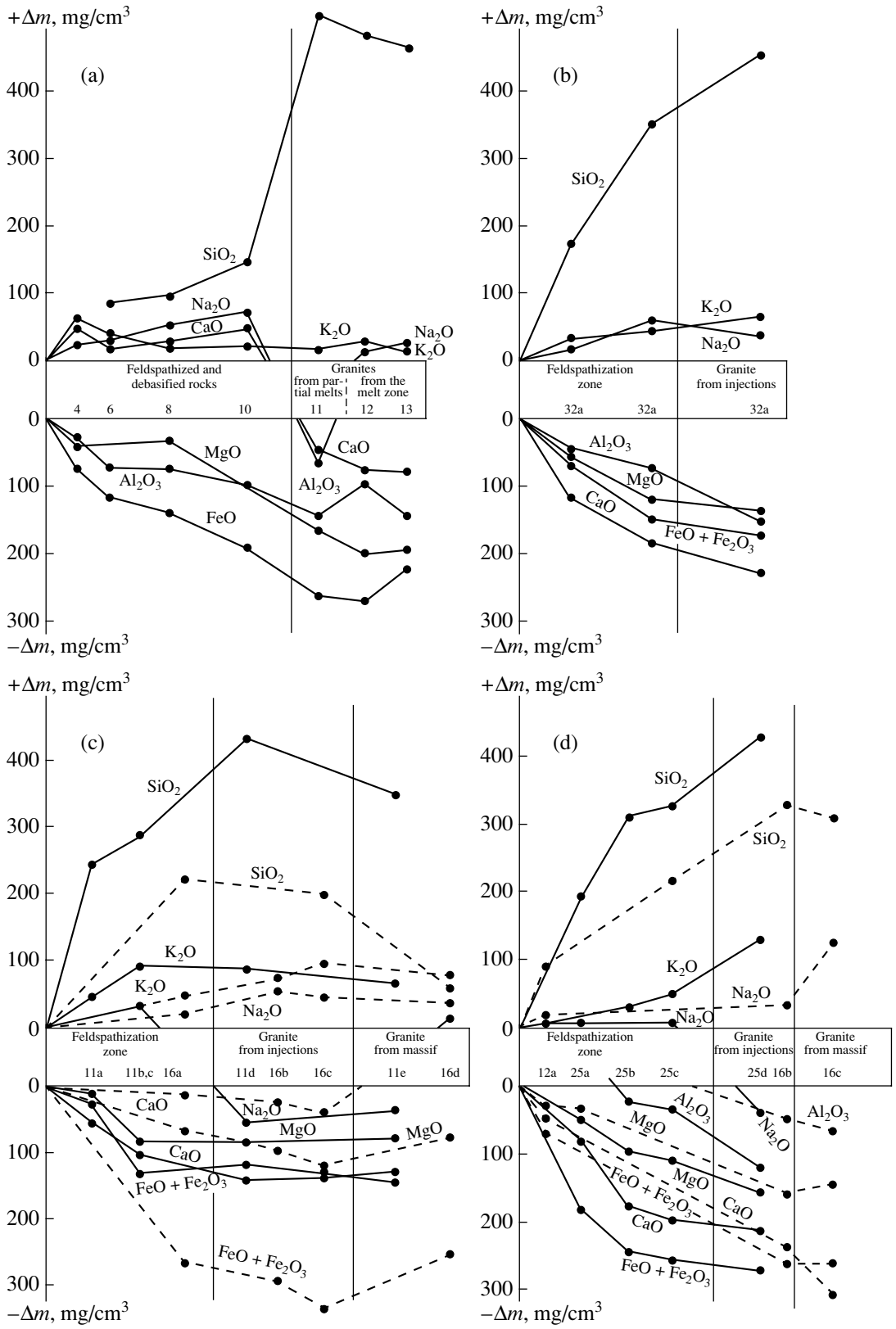

Fig. 10. Diagram showing the input (+Δ*m*) and output (–Δ*m*) of components (oxides) in the experimental and natural columns of granitization. (a) Experimental data reported in this paper. (b) Data on the natural columns of amphibolite granitization. (c) Data on granitization columns formed in biotite–clinopyroxene (solid line) and biotite–garnet (dashed line) gneisses. (d) Data on the granitization of basic granulites (pyroxene–plagioclase composition); the potassium and sodium lines of granitization are shown by solid and dashed lines, respectively.

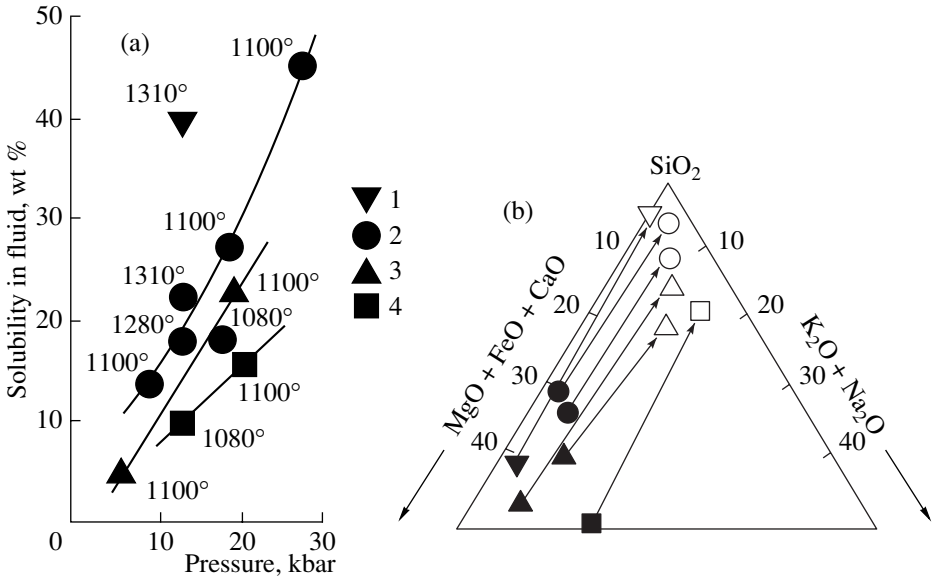

Fig. 11. (a) Solubility of model mantle materials in aqueous fluid and (b) compositions of initial materials (filled symbols) and components dissolved in fluid (unfilled symbols). (1) Enstatite, (2) peridotite and phlogopite peridotite, (3) basalt, and (4) phlogopite.

sule was kept under such pressure for 24 h before quenching.

After experiments without decompression, no changes were observed in the basalt powder and the plagioclase grain. The decompression experiments resulted in the formation of granitic glass, which partly replaced the plagioclase grain along its margin (Table 4). The interpretation of the experimental results is unequivocal. During the initial stage of the experiments (at 5 kbar and 730°C), fluid reacted with the basaltic material and was saturated in silica and alkalis primarily at the expense of the incongruent dissolution of basaltic minerals. During decompression, i.e., a pressure decrease from 5.0 to 2.0–3.5 kbar, the solubility of silica and alkalis in fluid decreased, which resulted in the formation of granitic melt, the solidus of which is lower than the experimental temperature (730°C), on the plagioclase grain.

One important property of the system should be pointed out. There is a fundamental difference between eutectic crystallization in dry and water-saturated systems. In a dry system, the maximum number of phases crystallize (or melt) at the eutectic point; in a binary system, two solid phases = melt (A + B = $L_{(AB)}$). In water-saturated systems, fluid plays a role of one or several phases: in our experiments, *Pl* + fluid (H_2O, SiO_2, K_2O, Na_2O) = $L_{(Pl + Kfs + Qtz)}$ + fluid (H_2O, CaO). Therefore, the replacement of monomineralic feldspar rocks in natural systems is nonisochemical eutectic crystallization, which is different from ordinary ("classic") eutectic crystallization. It can be referred to as the open-system eutectic. Strictly speaking, this is part of the evolution of the total system, which is terminated by the eutectic crystallization of the fluid-bearing system via the classic mechanism, but these parts are usually spatially separated in nature (open system).

MIGMATITES FORMED BY THE DIFFUSION MECHANISM

According to the generally accepted concept, the genesis of migmatites is related to the injection of granite melt or infiltration granitization. However, the experimental investigation of granite–amphibolite interaction revealed a new type of migmatites formed by the diffusion of silicon and alkalis into the contact aureole composed of amphibolite.

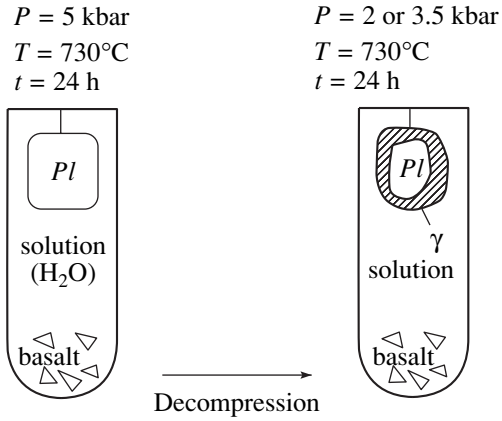

Fig. 12. A sketch and results of decompression experiments simulating effects caused by ascending mantle fluid. Abbreviations: *Pl*, plagioclase and γ, granite melt.

Table 4. Chemical compositions (wt %) of starting materials and granitic glasses obtained in the decompression experiments

Component	Basalt*	Pl_{51}	Glass, $P_f = 3.5$ kbar	Glass, $P_f = 2.0$ kbar
SiO_2	50.86	55.41	74.30	74.61
Al_2O_3	12.40	27.75	16.20	17.52
FeO	6.95	0.22	0.23	0.38
MgO	9.14	0.06	0.19	0.47
CaO	12.50	10.40	0.66	0.58
Na_2O	2.70	5.46	4.50	4.04
K_2O	9.50	0.26	3.44	2.35

* Basalt also contains 1.00 wt % TiO_2, 2.73 wt % Fe_2O_3, 0.14 wt % MnO, and 0.94 wt % H_2O.

We performed several experiments simulating interaction between granitic melt and amphibolites in the presence of fluid. The design of these experiments was the following. Finely powdered amphibolite (200–300 mg) was packed into the bottom of a gold capsule, after which water (40–50 ml) or solution (H_2O + 0.2 M HCl or H_2O + 0.5 M KCl) was added. Granite glass (200–300 mg) was then loaded and also tightly packed. The capsule was welded shut and held for 3–4 d at experimental conditions of $P = 7$ kbar and $T = 800$ and 950°C. The experimental products were examined with an optical microscope and electron microprobes (Camebax at the Institute of Experimental Mineralogy, Russian Academy of Sciences, and CamScan with an EOS Link system at Moscow State University).

The amphibolites were extensively altered in both experimental series (at 800 and 950°C). Their initial minerals ($Pl_{30} + Hbl_{45} + Bt_{42}$) were replaced by a more calcic plagioclase (up to Pl_{50}), more magnesian biotite and hornblende, clinopyroxene, and droplets and pockets of granite melt. The amount of melt increased toward the contact with the granite, where it formed migmatites-like veinlets and pockets. The analysis of data from several experiments allowed us to summarize the transformations as the following schemes based on the microprobe determination of mineral compositions:[3]

800°C, 7 kbar

0		1a		2a		3a
$Pl_{30} + Hbl_{45} + Bt_{42}$	⟶	$Pl_{35\to46} + Hbl + Bt_{43} + L^{24–33}$	⟶	$Hbl + Bt_{43} + Bt_{46} + L^{67–76}$	⟶	L^{100}
initial amphibolite		altered amphibolite		migmatites		granite

950°C, 7 kbar

0		1b		2b		3b		
$Pl_{30} + Hbl_{45} + Bt_{42}$	⟶	$Pl_{30\to55} + Hbl + Cpx_{25} + Bt_{44} + L^{38}$	⟶	$Hbl + Cpx_{26} + Bt_{43} + L^{38–67}$	⟶	$Opx_{26} + Cpx + L^{83}$	⟶	L^{100}
initial amphibolite		altered amphibolite		migmatites		granite		

It can be seen from Fig. 13 that the content of SiO_2 increases sharply with increasing amount of granitic melts. This is most clearly seen from a comparison with the composition of a granite veinlet (Fig. 13, analysis 33; Khodorevskaya and Zharikov, 2001). All samples (average compositions) show a decrease in Al_2O_3, MgO, and FeO concentrations and an increase in Si/Al and MgO/FeO ratios toward the contact with granite. The concentration of CaO shows minor variations and decreases in the granite. The concentration of Na also changes weakly, whereas that of K increases significantly.

Figure 13 presents the average compositions of particular areas in migmatized amphibolites (except for analysis 33). In fact, they are rather heterogeneous: areas of granitic melt (analysis 33) alternate with restites, which are almost always more mafic than the initial amphibolites and composed of more magnesian biotites and hornblendes (clinopyroxene is formed at 950°C) and more calcic plagioclases. The presence of more basic restites is an important feature distinguishing this migmatites type from infiltration varieties, in which the remains of amphibolites are always more silicic than the initial rocks.

The continuous changes in chemical composition and variable compositions of minerals in alteration zones unambiguously indicate the diffusion character of fluid-assisted interaction between granite and amphibolite.

Note also that similar alteration zones differing only in some minor structural and compositional characteristics were obtained in experiments performed at differ-

[3]The subscripts of mineral symbols indicate typical compositions and ranges of their variations; for instance, $Bt_{43–25}$ denotes biotite with 100Fe/(Fe + Mg) between 43 and 25. The superscripts indicate variations in the amount of the phase; for instance, $L^{38–67}$ means that the amount of melt in the zone ranges from 38 to 67 vol %.

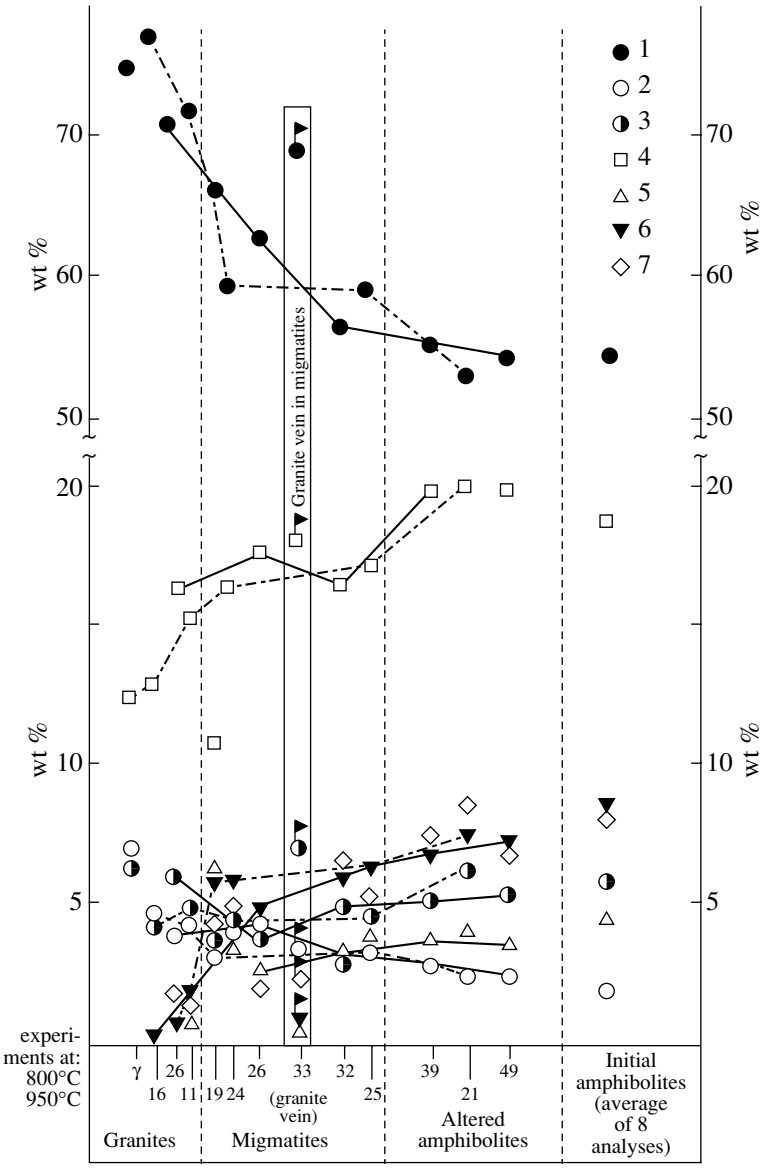

Fig. 13. Results of experiments on the contact interaction of granite melt with amphibolites in the presence of fluid. The average compositions of zones are shown for 800°C (solid line) and 950°C (dash–dot line). (1) SiO_2, (2) K_2O, (3) Na_2O, (4) Al_2O_3, (5) MgO, (6) FeO, and (7) CaO.

ent temperatures and with different solutions: H_2O (800 and 950°C), H_2O + 0.2 M HCl (800 and 950°C), and H_2O + 0.5 M KCl (950°C). In the 950°C experiments, the zone of interaction was distinguished by a more intense alteration of amphibolites, appearance of clinopyroxene in the residue, more aluminous hornblende composition, significantly higher amounts of granite melts, and presence of charnockitic assemblages in the boundary melt zone. In the presence of K-bearing fluid, the biotite, melt, and even hornblende were enriched in K. The compositions and assemblages of interaction zones were described in more detail by Khodorevskaya and Zharikov (2001) and Zharikov and Khodorevskaya (2004).

CONCLUSIONS

Summing up the diverse evidence obtained in our experimental investigations of granite formation after amphibolites, the following fundamentally new points should be highlighted.

(1) At 8–25 kbar both under dry conditions and in the presence of water, the partial melting of olivine-normative amphibolite produces trondhjemite–tonalite and granite–granodiorite liquids. This implies that silica-rich melts can be generated from metamorphosed mantle-derived basalts under lower crust conditions in subduction zones. The composition of such melts depends

mainly on temperature (degree of melting) and pressure.

(2) The influence of apoamphibolite silicic melts and their fluids ascending from the subduction zone on the overlying mantle wedge results in the formation of andesitic magmas, which can be regarded as prototypes of possible centers of island-arc magmatism.

(3) Under high *P–T* conditions, mantle fluids contain considerable amounts of silica and alkalis. A decrease in pressure and temperature promotes fluid interaction with the aluminosilicate material of basalts, which results in the formation of granitoid melts. It can be supposed that primary granites are formed in the basaltic crust owing to the autogranitization of basalts by mantle fluids.

(4) The column of infiltration granitization of amphibolites was experimentally reproduced. It consists of several metasomatic zones of debasification and feldspathization: a zone of feldspar-dominated rocks with melt lenses and veinlets (migmatization zone) and a zone of complete replacement of altered rocks with granitic melt (magmatic replacement). These experiments confirmed and elucidated the mechanism of "granitization as a magmatic replacement," which was first proposed by Korzhinskii and studied in detail by us and other researchers in many natural complexes. The granitization of schists and gneisses occurred on a greater scale and resulted in the formation of large massifs of granites and granitized rocks.

(5) Fluids must be considered as a eutectic phase during infiltration granitization. In such a way, a physicochemical explanation was provided for the replacement of monomineralic feldspar rocks by melt: feldspar + fluid = eutectic granitic melt. Therefore, the concept of eutectic in natural systems must include fluid components.

(6) It was experimentally shown that migmatization can occur by a diffusion mechanism in contact with granite veins or massifs as a result of the diffusion of silica and to some extent alkalis in aqueous fluids released from the granite bodies into the country rocks. The fluids interact with the country rocks causing their melting and development of pockets and veinlets of granite composition forming migmatites. The latter are accompanied by restites with a more basic composition compared with the minerals of the country rocks: more calcic plagioclases and more magnesian biotite and hornblende. In this respect they are different from infiltration migmatites, which are always accompanied by the debasification of the country rocks. On the other hand, part of Ca, Mg, and Fe diffuses into the granitic melt forming a more basic boundary zone of granitoid.

ACKNOWLEDGMENTS

The authors are grateful to their colleagues who contributed to these studies. Special thanks are due to V.M. Shmonov (Institute of Experimental Mineralogy, Russian Academy of Sciences), who developed a new method for the investigation of fluid–magma infiltration processes. We express our gratitude to A.Yu. Bychkov and E.A. Solopova (Moscow State University) for the assistance in the preparation of the manuscript for publication. This study was financially supported by the Russian Foundation for Basic Research (project nos. 05-05-64166 and 06-05-64645) and Theme no. 9 of the Program of the Department of Earth Sciences, Russian Academy of Sciences.

REFERENCES

1. F. Barker and J. G. Arth, "Generation of Trondhjemitic–Tonalitic Liquids and Archean Bimodal Trondhjemite–Basalt Suites," Geology, No. 4, 596–600 (1976).
2. J. S. Beard and G. E. Lofgren, "Dehydration Melting and Water-Saturated Melting of Basaltic and Andesitic Greenstones and Amphibolites at 1, 3 and 6.9 kb," J. Petrol. **32**, 365–402 (1991).
3. D. H. Eggler, "Upper Mantle Oxidation State: Evidence from Olivine–Orthopyroxene–Ilmenite Assemblages," Geophys. Res. Lett. **10**, 365–368 (1983).
4. R. T. Flynn and C. W. Burnham, "An Experimental Determination of Rare Earth Partition Coefficient between a Chloride Containing Vapor and Silicate Melt," Geochim. Cosmochim. Acta **42**, 685–701 (1978).
5. T. Gasparik, "Experimental Study of Subsolidus Phase Relations and Mixing Properties of Pyroxene in the system $CaO–Al_2O_3–SiO_2$," Geochim. Cosmochim. Acta **48**, 2537–2545 (1984).
6. T. Gasparik, "Experimental Study of Subsolidus Phase Relations and Mixing Properties of Clinopyroxene in the System $CaO–MgO–Al_2O_3–SiO_2$," Am. Mineral. **71**, 686–693 (1986).
7. S. N. Gavrikova and V. A. Zharikov, "Geochemical Features of Archean Rock Granitization in Eastern Transbaikalia," Geokhimiya, No. 1, 26–49 (1984).
8. N. S. Gorbachev, *Fluid–Magma Interaction in Sulfide–Silicate Systems* (Nauka, Moscow, 1989) [in Russian].
9. B. R. Hacker, "Amphibolite-Facies-to-Granulite-Facies Reactions in Experimentally Deformed, Unpowdered Amphibolite," Am. Mineral. **75**, 1349–1361 (1990).
10. A. Irving, "A Review of Experimental Studies of Crystal/Liquid Trace Element Partitioning," Geochim. Cosmochim. Acta **42**, 743–770 (1978).
11. L. T. Khanukhova, V. A. Zharikov, and Yu. A. Litvin, "Excess Silica in High-Pressure Clinopyroxene Solid Solutions According to an Experimental Study of the System $CaMgSi_2O_6–CaAl_2SiO_6–SiO_2$ at P = 35 kbar and T = 1200°C," Dokl. Akad. Nauk SSSR **229**, 23–26 (1976a).
12. L. T. Khanukhova, V. A. Zharikov, and Yu. A. Litvin, "Pyroxene Solid Solutions in the System $NaAlSi_2O_6–CaAl_2SiO_6–SiO_2$ at P = 35 kbar and T = 1200°C," Dokl. Akad. Nauk SSSR **231**, 185–187 (1976b).
13. L. I. Khodorevskaya and V. A. Zharikov, "Experimental Simulation of Amphibolite and Ultrabasic Rock Interaction in Subduction Zones," Petrologiya **5**, 4–9 (1997) [Petrology **5**, 2–7 (1997)].

14. L. I. Khodorevskaya and V. A. Zharikov, "Experimental Study of Amphibolite Partial Melting at Different Compositions of the Fluid Phase," Dokl. Akad. Nauk **359**, 536–539 (1998a) [Dokl. Earth Sci. **359A**, 416–419 (1998)].
15. L. I. Khodorevskaya and V. A. Zharikov, "Experimental Study of Amphibolite Melting and the Genesis of Tonalite-Trondhjemite Magmatic Series," in *Experimental and Theoretical Modeling of Mineral Formation* (Nauka, Moscow, 1998b), pp. 11–31 [in Russian].
16. L. I. Khodorevskaya and V. A. Zharikov, "Experimental Study of Interaction between Amphibolite and Granite Melt at 800–950°C and 7 kbar," Petrologiya **9**, 339–350 (2001) [Petrology **9**, 291–301 (2001)].
17. L. I. Khodorevskaya, V. M. Shmonov, and V. A. Zharikov, "Granitization of Amphibolite: Experimental Modeling at 750°C and 5 kbar Pressure," Dokl. Akad. Nauk **382**, 244–247 (2002) [Dokl. Earth Sci. **383**, 218–221 (2002)].
18. L. I. Khodorevskaya, V. M. Shmonov, and V. A. Zharikov, "Granitization of Amphibolites. 1. Results of First Experiments with Fluid Filtering through Rock," Petrologiya **11**, 321–331 (2003) [Petrology **11**, 291–300 (2003)].
19. D. S. Korzhinskii, "Granitization as a Magmatic Replacement," Izv. Akad. Nauk SSSR, Ser. Geol., No. 2, 56–69 (1952).
20. B. O. Mysen and I. Kushiro, "Compositional Variation of Coexisting Phases with Degree of Melting of Peridotite under Upper Mantle Conditions," Carnegie Inst. Wash. Yearb. **75**, 546–555 (1976).
21. Y. Nakamura and I. Kushiro, "Composition of the Gas Phase in Mg_2SiO_4–SiO_2–H_2O at 45 kbar," Carnegie Inst. Wash. Yearb. **73**, 255–258 (1974).
22. R. P. Rapp, E. B. Watson, and C. F. Miller, "Partial Melting of Amphibolite, Eclogite and the Origin of Archean Trondhjemites and Tonalites," Precambrian Res. **51**, 1–25 (1991).
23. T. Rushmer, "Partial Melting of Two Amphibolites under Fluid-Absent Conditions," Contrib. Mineral. Petrol. **107**, 41–59 (1991).
24. I. D. Ryabchikov, "Mobilization of Ore Metals in Acid Magmatic Systems (Experimental Data)," in *Endogenous Ore Formation* (Nauka, Moscow, 1985), pp. 95–100 [in Russian].
25. I. D. Ryabchikov and A. L. Boettcher, "Composition of Fluids in Equilibrium with Phlogopite-Bearing Mantle Assemblages under High Temperatures and Pressures," Izv. Akad. Nauk SSSR, Ser. Geol., No. 3, 56–61 (1986).
26. N. V. Surkov and A. M. Doroshev, "Phase Diagram of the System CaO–Al_2O_3–SiO_2 at Pressures of up to 40 kbar," Geol. Geofiz. **39**, 1254–1268 (1998).
27. N. V. Surkov and G. N. Kuznetsov, "Experimental Study of Clinopyroxene Stability in the *Cpx* + *Opx* + *Gr* Assemblage, the CaO–MgO–Al_2O_3–SiO_2 System," Geol. Geofiz. **37** (12), 18–25 (1996).
28. A. B. Thompson, "Dehydration Melting of Pelitic Rocks and the Generation of H_2O-Undersaturated Granitic Liquids," Am. J. Sci. **282**, 1567–1596 (1982).
29. K. T. Winther and R. C. Newton, "Experimental Melting of Hydrous Low-K Tholeiite: Evidence on the Origin of Archean Cratons," Bull. Geol. Soc. Den. **39**, 213–228 (1991).
30. M. B. Wolf and P. J. Wyllie, "Crystal Settling in Hydrous Syenite Melt at 15 kbar," Geol. Soc. Am. Abstr. **18**, 200 (1986).
31. M. B. Wolf and P. J. Wyllie, "Dehydration Melting of Solid Amphibolite at 10 kb: Textural Development, Liquid Interconnectivity and Applications to the Segregation of Magmas," Mineral. Petrol. **44**, 151–179 (1991).
32. M. B. Wolf and P. J. Wyllie, "Garnet Growth during Amphibolite Anatexis: Implications of a Garnetiferous Restite," J. Geol. **101**, 357–373 (1993).
33. P. J. Wylle, "Magmas and Volatile Components," Am. Mineral. **64**, 464–500 (1979).
34. H. S. Yoder and C. E. Tilley, "Origin of Basalt Magmas and Experimental Study of Natural and Synthetic Rock Systems," J. Petrol. **3**, 342–532 (1962).
35. V. A. Zharikov, "Problems of Granite Formation," Vestn. Mosk. Univ., Ser. 4: Geol., No. 6, 3–14 (1987).
36. V. A. Zharikov, "Dehydration and Melting during Various Thermodynamic Water Regimes," Petrologiya **3**, 340–348 (1995a).
37. V. A. Zharikov, "Fluids in Geological Processes," in *Fluids in the Crust. Equilibrium and Transport Properties*, Ed. by K. I. Shmulovich and B. W. D. Yardley (Chapman–Hall, London, 1995b), pp. 13–41.
38. V. A. Zharikov, "Genesis of Granite Magmas," in *Selected Scientific Reports of RFBR*, pp. 55–57 (1996a).
39. V. A. Zharikov, "Some Aspects of the Granite Formation Problem," Vestn. Mosk. Univ., Ser. 4: Geol., No. 4, 3–13 (1996b).
40. V. A. Zharikov and S. N. Gavrikova, "Granite Formation at the Active Margin of the Aldan–Stanovoy Shield," Zap. Vseross. Mineral. O–va **116**, 377–399 (1987).
41. V. A. Zharikov and S. N. Gavrikova, "Two Mechanisms of Granite Formation," in *Proceedings of 27th International Geological Congress. Crystalline Crust in Space and Time, Moscow, Russia, 1984* (Nauka, Moscow, 1989), pp. 25–36 [in Russian].
42. V. A. Zharikov and L. I. Khodorevskaya, "Amphibolite Melting: *T–P* Relations of the Composition of Partial Melts," Dokl. Akad. Nauk **330**, 249–251 (1993).
43. V. A. Zharikov and L. I. Khodorevskaya, "Amphibolite Melting: Compositions of Partial Melts at 5–25 kbar," Dokl. Akad. Nauk **341**, 799–803 (1995).
44. V. A. Zharikov and L. I. Khodorevskaya, "Experimental Study of Amphibolite Melting with Applications to the Genesis of Tonalite–Trondhjemite Magmas," in *Experimental and Theoretical Modeling of Mineral Formation* (Nauka, Moscow, 1998), pp. 11–31 [in Russian].
45. V. A. Zharikov and L. I. Khodorevskaya, "Generation of Granites after Amphibolites: Experimental Study," in *Proceedings of All-Russian Scientific Conference on Geology, Geochemistry, and Geophysics at the Turn of 20th and 21th Centuries, Moscow, Russia, 2002* (Svyaz'-Print, Moscow, 2002), Vol. 2, p. 82 [in Russian].
46. V. A. Zharikov and L. I. Khodorevskaya, "Migmatization during Interaction of Fluid Granite Melts with Amphibolites: Experimental Study," in *Experimental Mineralogy. Some Results at the Turn of the Century* (Nauka, Moscow, 2004), Vol. 2, pp. 123–148 [in Russian].

47. V. A. Zharikov, R. A. Ishbulatov, and Yu. A. Litvin, "Calc-Alkaline Magmatic Melts under High (25–45 kbar) Pressures," in *Proceedings of All-Union Conference of Chemical Society* (Nauka, Moscow, 1975), No. 1, pp. 357–358 [in Russian].

48. V. A. Zharikov, V. A. Ishbulatov, and Yu. A. Litvin, "Influence of Alkaline and Fluid Components on the Genesis of Calc-Alkaline Magmas," in *Proceedings of 11th Conference of the International Mineralogical Association. Experimental Mineralogy* (Nauka, Moscow, 1980), pp. 22–33 [in Russian].

49. V. A. Zharikov, V. A. Ishbulatov, and L. T. Chudinovskikh, "Eclogite Barrier and High-Pressure Clinopyroxenes," Geol. Geofiz., No. 12, 54–63 (1984).

50. V. A. Zharikov, M. B. Epel'baum, and M. V. Bogolepov, "Experimental Study of the Possibility of Granitization under the Influence of Deep-Seated Fluids," Dokl. Akad. Nauk SSSR **331**, 462–465 (1990).

51. V. A. Zharikov, A. G. Simakin, and M. B. Epel'baum, "Modeling of the Generation of Granite Magmas by the Interaction of Basaltic Melts with Crustal Materials," Vestn. Mosk. Univ., Ser. 4: Geol., No. 2, 3–15 (1991).

52. V. A. Zharikov, M. B. Epel'baum, and M. V. Bogolepov, "Processes of Granite Formation," in *Experimental Problems in Geology* (Nauka, Moscow, 1994), pp. 83–103 [in Russian].